Biochimica et Biophysica Acta 1828 (2013) 2247–2254

Contents lists available at SciVerse ScienceDirect

Biochimica et Biophysica Acta

journal homepage: www.elsevier.com/locate/bbamem

Effect of melatonin and cholesterol on the structure of DOPC and DPPC membranes

E. Drolle [a,b], N. Kučerka [c,d], M.I. Hoopes [e], Y. Choi [a,b], J. Katsaras [c,f], M. Karttunen [b,e], Z. Leonenko [a,b,g,*]

[a] Department of Biology, University of Waterloo, Canada
[b] Waterloo Institute for Nanotechnology, University of Waterloo, Canada
[c] Canadian Neutron Beam Centre, Chalk River, Ontario, Canada
[d] Department of Physical Chemistry of Drugs, Comenius University, Slovakia
[e] Department of Chemistry, University of Waterloo, Canada
[f] Biology and Soft Matter Division, Oak Ridge National Laboratory, Joint Institute for Neutron Sciences, Oak Ridge, TN, USA
[g] Department of Physics and Astronomy, University of Waterloo, Canada

ARTICLE INFO

Article history:
Received 11 January 2013
Received in revised form 17 May 2013
Accepted 17 May 2013
Available online 25 May 2013

Keywords:
Lipid membrane
Cholesterol
Melatonin
Small-angle neutron diffraction (SAND)
Small-angle neutron scattering (SANS)
Molecular Dynamics simulations

ABSTRACT

The cell membrane plays an important role in the molecular mechanism of amyloid toxicity associated with Alzheimer's disease. The membrane's chemical composition and the incorporation of small molecules, such as melatonin and cholesterol, can alter its structure and physical properties, thereby affecting its interaction with amyloid peptides. Both melatonin and cholesterol have been recently linked to amyloid toxicity. Melatonin has been shown to have a protective role against amyloid toxicity. However, the underlying molecular mechanism of this protection is still not well understood, and cholesterol's role remains controversial. We used small-angle neutron diffraction (SAND) from oriented lipid multi-layers, small-angle neutron scattering (SANS) from unilamellar vesicles experiments and Molecular Dynamics (MD) simulations to elucidate non-specific interactions of melatonin and cholesterol with 1,2-dioleoyl-*sn*-glycero-3-phosphocholine (DOPC) and 1,2-dipalmitoyl-*sn*-glycero-3-phosphocholine (DPPC) model membranes. We conclude that melatonin decreases the thickness of both model membranes by disordering the lipid hydrocarbon chains, thus increasing membrane fluidity. This result is in stark contrast to the much accepted ordering effect induced by cholesterol, which causes membranes to thicken.

1. Introduction

The cell membrane is the first line of defense against invading species, and is key to understanding disease, including amyloid toxicity that is commonly associated with Alzheimer's disease. Small molecules, such as cholesterol and melatonin incorporate into the lipid matrix and are known to alter the membrane's structure and physical properties [1,2]. These changes to the membrane subsequently affect its functionality and its interactions with biomolecules. While the interaction of cholesterol with membranes has been extensively studied, the effect of melatonin on the structure of lipid membranes is not well understood. Structural studies detailing the effects of melatonin and cholesterol on membranes are, however, of great importance because both molecules have been linked to amyloid toxicity associated with Alzheimer's disease.

Alzheimer's (AD) is a neurodegenerative disease and a major form of dementia that becomes more prevalent with increasing age. AD is associated with the formation of plaques and insoluble amyloid fibrils, which are composed of amyloid-beta (Aβ) proteins folded into β-sheets, and which are found on the surface of neuronal plasma membranes [3]. Recent studies have shown the lipid membrane to be extremely important in enabling amyloid fibril formation and its ensuing toxicity [4–6].

In both human and animal studies melatonin has been shown to have a protective role against AD, namely slowing the progress of the disease [7–10]. However, the underlying molecular mechanism of this protective effect is not well understood. Melatonin is a pineal hormone that is produced in the human brain and is responsible for maintaining the circadian rhythm and regulating the sleep–wake cycle [11]. In addition to its well-known anti-oxidative effects, melatonin is known for its involvement in intracellular signal transduction, regulation of cell death and cell proliferation [12]. The protective mechanism of melatonin against AD may involve a nonspecific interaction of the molecule with the membrane [1]- although its effects on lipid membranes remain inconclusive and controversial. It has also been reported that melatonin decreases the gel-to-fluid phase transition temperature in a number of different lipid systems, implying that melatonin increases membrane disorder [1,13–16]. In contrast, slower membrane dynamics have been reported in DPPC bilayers [1], rat brain homogenate [17,18], and in DMPC membranes [15,19]. Garcia et al. reported on the stabilizing

* Corresponding author at: Department of Physics and Astronomy, University of Waterloo, Canada. Tel.: +1 519 888 4567.
E-mail address: zleonenk@uwaterloo.ca (Z. Leonenko).

0005-2736/$ – see front matter © 2013 Elsevier B.V. All rights reserved.
http://dx.doi.org/10.1016/j.bbamem.2013.05.015

effect of melatonin in synergy with other drugs on mitochondrial membrane [20]. These important, but somewhat contradictory results therefore necessitate further studies regarding melatonin's effects on biologically relevant membrane systems.

Although a number of in vitro studies have demonstrated the above-mentioned protective effects of melatonin against Aβ, including studies at the cellular level [10,21,22], the underlying mechanisms of melatonin's protective action have yet to be adequately explained. For example, Galano et al. emphasized the importance of the antioxidant action of melatonin [23]; Bongiorno et al. have shown that melatonin may compete with cholesterol for binding to lecithin, and that it may even displace cholesterol from the phospholipid bilayer [2]. Melatonin's ability to control cholesterol content, ergo membrane rigidity, may thus reduce the effects of cholesterol on the membrane, as well as cholesterol-mediated processes [9]. Previous studies [1–9,11–13,15,16] have demonstrated melatonin's ability to non-specifically bind to and interact with the lipid membrane, and to alter its biophysical properties. In addition to its antioxidative protection, the biophysical effects of melatonin on the membrane may also contribute to its cell protective qualities and thus deserve further investigation. In this study we specifically focus on the non-specific biophysical effect of melatonin on model membranes with the purpose of comparing it to the effect by cholesterol.

In contrast to melatonin's protective abilities, it has been shown that cholesterol, when in a membrane, can enhance amyloid binding and fibril formation [24]. However, depending on the type of lipid and amyloid peptide, others have reported that cholesterol hinders the insertion of amyloid peptides into lipid membranes [25]. We have recently shown that cholesterol induces non-homogeneous binding of the amyloid peptide to the lipid membrane, resulting in the formation of membrane defects [26]. Sheikh et al. also reported enhanced membrane solubilization and defect formation when cholesterol was present in model membranes [27]. On the cellular level, cholesterol has been shown to reduce the toxic effect of amyloid plaques on neuroblastoma cells [28]. Therefore, in order to better understand how melatonin and cholesterol affect the interaction of biomolecules – e.g., amyloid fibrils – with the membrane, it is necessary to systematically determine the effects that these molecules have on membrane structure.

Cholesterol is a well-known sterol that usually orients itself parallel to bilayer lipids, the exception being in bilayers with polyunsaturated fatty acids, where cholesterol sequesters into the middle of the bilayer (i.e., orthogonal to the bilayer normal) [29]. According to the lipid raft hypothesis, cholesterol is an important constituent of lipid rafts [30–34]. Rafts saturated with cholesterol and sphingolipids, as well as saturated lipids such as 1,2-dipalmitoyl-*sn*-glycero-3-phosphocholine (DPPC), are thought to compartmentalize certain cellular processes, including cell signaling, molecular assembly and membrane protein trafficking, and require the presence of cholesterol in order to form [31,32,35]. Cholesterol has also been shown to affect membrane permeability and fluidity, as well as the mechanical properties of model membranes [31,32,36–38]. Factors affecting cholesterol's influence on membranes include its concentration and membrane composition [32,39,40].

Neutron scattering has been extensively used to study the structure of model lipid membranes. The technique has been employed to accurately determine bilayer structural parameters (e.g., lipid area, bilayer thickness), cholesterol's location in multilayers, and its interactions with different lipids, to name a few [41–45]. To the best of our knowledge, neutron scattering has not been previously used to study the effect of melatonin on model membranes, nor how cholesterol's effects on membranes differ from those of melatonin. Moreover, there are no computer simulation studies of the effect of melatonin on membranes. We believe this to be the first study to address the molecular mechanisms of melatonin–lipid and melatonin–cholesterol–lipid interactions using Molecular Dynamics (MD) simulations in comparison with neutron scattering experiments.

2. Materials and methods

2.1. Sample preparation

1,2-Dipalmitoyl-*sn*-glycero-3-phosphocholine (DPPC), 1,2-dioleoyl-*sn*-glycero-3-phosphocholine (DOPC), melatonin and cholesterol were purchased from Sigma-Aldrich (St. Louis, MO) in powder form. All other chemicals used were of reagent grade.

Lipids were solubilized in a 1:1 solution of chloroform: TFE (trifluoroethanol) with the requisite amount of cholesterol or melatonin (reported here in molar fractions) placed in a glass vial at total lipid concentrations of between 25 and 30 mg/mL. Approximately 15 mg of pure lipid; a mixture of lipid and cholesterol; or a mixture of lipid and melatonin (thin film thickness of ~0.001 cm when spread onto a 25 × 60 mm^2 silicon wafer), was deposited onto a silicon wafer and rocked during evaporation of the organic solvent in a glove box to form samples of highly oriented multilayer stacks [46]. The remaining solvent was removed by placing the oriented samples under vacuum prior to diffraction measurements.

Samples of unilamellar vesicles (ULVs) were prepared for study by small angle neutron scattering (SANS). Lipids were mixed with cholesterol/melatonin in chloroform, and then solutions were dried, initially in a stream of inert gas (e.g., Ar or N_2), and subsequently under vacuum. The resulting lipid film was hydrated using the requisite amount of 100% D_2O resulting in a solution with a total lipid concentration of 20 mg/mL. The dispersions of self-assembled multilamellar vesicles (MLVs) were then extruded through polycarbonate filters populated with 50 nm pores using an Avanti Extruder (Avanti Polar Lipids, Alabaster, AL). This procedure has been shown to yield reasonably monodisperse ULVs with a mean diameter of ~60 nm [47].

2.2. Small-angle neutron diffraction

Neutron diffraction data were collected at the Canadian Neutron Beam Centre's (CNBC) N5 beamline, which is located at the National Research Universal (NRU) reactor (Chalk River, Ontario, Canada). Neutrons of 0.237 nm wavelength were selected by the (002) reflection of a pyrolytic graphite (PG) monochromator, and a PG filter was used to eliminate higher order reflections. Incoming neutrons were collimated into a rectangular beam of dimensions 6 × 50 mm^2, and scattering angles were determined via the sample angle θ and the detector angle Φ. Samples were placed in an airtight sample cell and hydrated with saturated K_2SO_4 (97% relative humidity) solutions using a series of different neutron contrast D_2O/H_2O mixtures (i.e., 70%, 40%, and 8% D_2O) at 25 °C.

Sample stability over the duration of the experiment was confirmed through the reproducibility of the diffraction data, whereby lamellar repeat spacings and peak intensities (i.e., for a given quasi-Bragg reflection) remained constant, indicating that bilayer structure was unaltered. Alignment quality for each sample was assessed using the Gaussian width of rocking curves (i.e., the sample was rotated through an angle θ, while the detector remained fixed at a given angle (Φ)). Fig. 1 shows a typical rocking curve with a sharp central peak (mosaic spread of Gaussian width ~0.05°) corresponding to large lateral domains of highly oriented multi-bilayers [48]. This narrow peak sits atop a broad peak (Gaussian width ~0.5°) consisting of scattering from much smaller domains with a broader distribution of orientations [49].

Diffraction curves were obtained using θ–2θ scans, i.e., where the detector is always positioned at $\Phi = 2\theta$. Typically five quasi-Bragg orders were detected, which were fitted to Gaussians and an additional second-order polynomial function associated with the background. Integrated intensities for the different quasi-Bragg peaks were corrected for incident neutron flux, sample absorption and the Lorentz correction, as described elsewhere [48]. The phases of the corrected form factors were deduced through the systematic substitution of H_2O by D_2O in the hydrating solution, whereby the bilayer form factors measured at different contrast

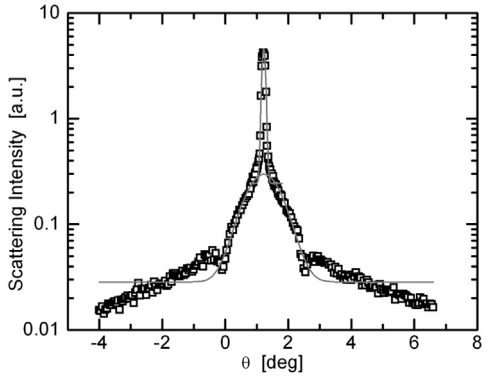

Fig. 1. Semi-log plot of a rocking curve (points) corresponding to the first order diffraction peak from aligned multi-bilayers (DOPC with 9 mol% melatonin). The width of the peak (gray lines) indicates the quality of the sample's alignment. Note that the neutron signal drops at two locations along the curve, both as a result of increased neutron absorption, which occurs when the sample is parallel to the incident (i.e., $\theta = 0$) or the diffracted (i.e., $\theta = \Phi$) neutron beam.

conditions change linearly as a function of D_2O content [50]. Finally, Neutron Scattering Length Density (NSLD) profiles were calculated via the Fourier transform of the scattering form factors, while absolute scale NSLD profiles were not determined. This procedure results in NSLD profiles that can be used to determine the characteristic features of bilayers. Moreover, the profiles obtained for samples hydrated with 8% D_2O solution show only the bilayer, and are not obscured from scattering by the solvent (in 8% D_2O the water contribution to the NSLD is practically zero). These profiles are thus best used to extract the membrane's fine structural details (i.e., lipid head-groups peak–peak distance across the bilayer, D_{HH}).

2.3. Small-angle neutron scattering

Neutron scattering data were collected at CNBC's N5 triple-axis spectrometer, which was adapted for SANS measurements [51], and at the CG-3 Bio-SANS instrument [52] located at Oak Ridge National Laboratory (ORNL). In the case of the N5 instrument, 4 Å wavelength neutrons were selected using a PG monochromator, and the scattered neutrons were detected using a 32 wire detector positioned at five predetermined angles (i.e., $\Phi = 1.5$, 3.3, 5.1, 6.9, and 8.7) covering a scattering range of 0.008 $Å^{-1} < q < 0.270$ $Å^{-1}$. In the case of the CG-3 instrument, 6 Å wavelength neutrons were selected using a mechanical velocity selector, and two different sample-to-detector distances (i.e., 2.5 and 15.3 m) were used, covering a total scattering vector of 0.004 $Å^{-1} < q < 0.370$ $Å^{-1}$. The two different experimental setups provided data of comparable quality (see Fig. 2), although the dedicated CG-3 instrument resulted in higher quality high q data.

SANS measurements were carried out using ULVs dispersed in a 100% D_2O solution — as opposed to H_2O. D_2O is often used in neutron experiments in order to decrease the large incoherent scattering that results from hydrogen atoms, and to increase the contrast between the hydrating water and the lipid bilayer — which is also rich in hydrogen. As a result, the system is best described by a three component strip model made up of pure water (outside the lipid bilayer), a bilayer core of pure hydrocarbons, and a region where the lipid head-groups are inter-dispersed with water. This type of strip model analysis [53] has been used successfully to study the effect of cholesterol on DOPC bilayers [38]. However, in the present study we substituted the sharp interfaces separating the adjacent strips with smooth error functions that represent a more realistic picture of membranes [54]. As a result, we report a bilayer thickness that corresponds to the steric thickness of the bilayer. It should be noted that this thickness is different from the D_{HH} obtained from SAND (described above), and is thus more appropriate to focus on the relative changes taking place within these

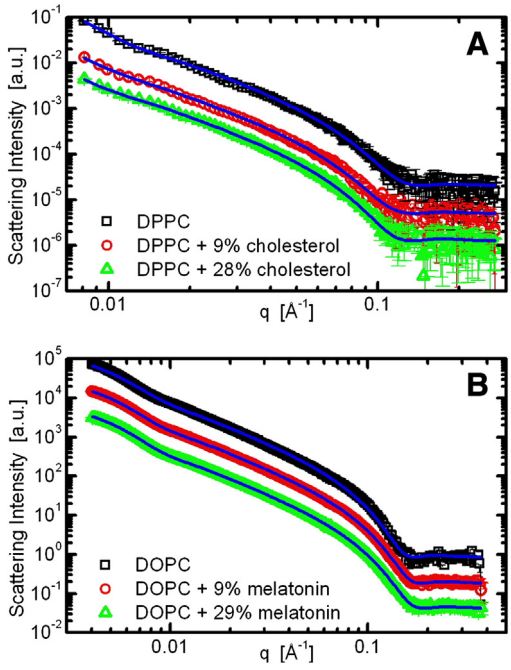

Fig. 2. Log–log plot of SANS data obtained for A) DPPC bilayers doped with different amounts of cholesterol (data from the N5 instrument) and B) DOPC bilayers doped with melatonin (measured on the CG-3 Bio-SANS instrument). The blue solid lines are best fits to the data (open symbols). The SANS curves are shifted from each other (by a factor of 4) for better visualization.

different membrane thickness parameters, rather than their absolute values.

2.4. Computational membrane modeling

We modeled phospholipid membranes with melatonin using atomistic MD simulations. Each system was composed of 512 lipid molecules, approximately 28,000 water molecules were added to achieve full hydration, along with 72 molecules of melatonin (for 12 mol%). The GROMACS software package [55] with the GROMOS 53a6 force-field [56] was used in the simulations. The GROMOS 53a6 force-field was used because it has been tested and validated for lipid and peptide systems [57,58]. Corrections by Bachar et al. were used for acyl double bonds as they have been shown to be important for proper modeling of sterol–lipid interactions [59]. New partial charges were determined for melatonin by quantum mechanical calculations using the Firefly (PC GAMESS) 7.1.G program [60]. The final parameterization of melatonin was computed using restricted Hartree–Fock type self-consistent field calculations in order to find the optimal starting geometry, as well as the partial charges. A Pople split valence basis set with 6 primitive Gaussians for the atomic cores, along with a combination of two basis functions to form valence orbitals comprised of 3 primitive Gaussians for the first valence orbital and 1 primitive Gaussian for the second orbital were used. A single polarization function was added to both heavy and light atoms (6-31dp), and the simple point charge (SPC) model was used for water. Bond lengths were constrained using the SETTLE [61] algorithm for water, and LINCS [62] for the lipids. Lennard-Jones interactions were treated with a switching algorithm that started at 0.8 nm and used a cutoff of 0.9 nm. Electrostatics were treated with the particle-mesh Ewald method [63,64] using a real space cutoff of 1.4 nm, beta spline interpolation (of order 4), and a direct sum tolerance of 1E-6. Periodic boundaries were used in all three dimensions, along with a 2 fs time step. The systems were set up by arranging 64 lipids per leaflet on a rectangular lattice. Steepest decent energy minimization was done before adding water, and then repeated. This was followed by a 100 ps NVT relaxation at 273.15 K using a

stochastic dynamics integrator and a 100 ps NpT relaxation at 300 K. For DPPC, a further relaxation (far above Tm =314 K) was carried out at 410 K for 20 ns before returning to 300 K. A final relaxation of 100 ns NpT simulation was carried out at 300 K and 1 bar. The production simulations were conducted in the NpT ensemble. Pressure and temperature were fixed at 1 bar and 300 K, respectively, using the Parrinello–Rahman algorithm [65] with a relaxation time of 0.5 ps, in the case of pressure, and the Parrinello–Donadio–Bussi v-rescale algorithm [66] for temperature coupling with a relaxation time of 0.1 ps. The temperatures of the lipids and water were coupled independently. This simulation protocol has been shown to be reliable for membranes and other related systems [57].

3. Results and discussion

In order to determine how melatonin affects membrane structure, and to compare these changes to those induced by cholesterol, we created a model of simplified bilayers containing either melatonin or cholesterol. It is well known that cholesterol when incorporated into a lipid bilayer partitions into the hydrocarbon chain region with its hydrophilic hydroxyl head-group residing in close proximity to the lipid head-groups [67–69] (Fig. 3A). It has also been proposed that melatonin may integrate itself into the head-group region of the lipid bilayer [16], as shown in Fig. 3B.

Our SAND data obtained from oriented stacks of multi-bilayers, and SANS data from ULV dispersions provide a more detailed description of the changes in bilayer structure incurred by the incorporation of cholesterol or melatonin into a lipid bilayer.

Fig. 4 shows the NSLD profiles of lipid bilayers obtained from SAND measurements. In the case of these samples, varying amounts of cholesterol, or melatonin, were added (in equivalent molar ratio amounts), and the samples were hydrated using solutions with different neutron contrasts. The 8% D_2O solution results in NSLD profiles whose scattering can be exclusively attributed to the lipid bilayer, with no contribution from the bulk water.

The bilayer thickening effect as a result of cholesterol is well documented [38,48,50,69] and our results (Fig. 4A and B) are in good agreement with previous published data. Fig. 4A and B clearly illustrate the changes taking place in the lipid head-group peak-to-peak distance (D_{HH}) as a function of increasing amounts of cholesterol in DOPC (Fig. 4A) and DPPC (Fig. 4B) bilayers. D_{HH} is a good indicator of bilayer thickness and corresponds to the distance separating head groups from opposing bilayer leaflets. It is clear that D_{HH} progressively increases with increasing amounts of cholesterol in the case of both bilayers (Fig. 4A and B). Although cholesterol does not initially result in any significant change to D_{HH}, this change becomes more pronounced with increasing amounts of cholesterol. In the absence of cholesterol, the D_{HH} of the DOPC bilayer (Fig. 4A) is 33.9 Å, and increases to 34.7 Å and 37.1 Å at 9% and 29% cholesterol, respectively. A similar trend of increasing thickness is seen in DPPC bilayers (Fig. 4B): D_{HH} of the pure DPPC bilayer is 39.2 Å, and increases to 39.4 Å and 44.8 Å at 9% and 28% cholesterol, respectively.

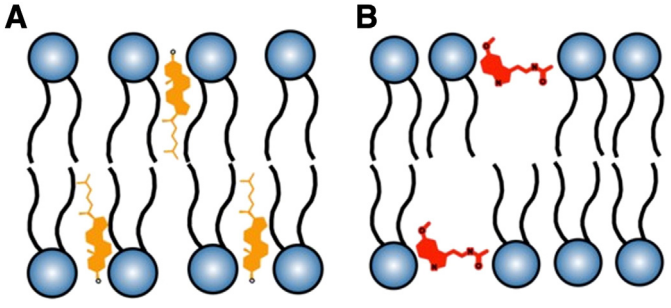

Fig. 3. Schematics illustrating the proposed locations of cholesterol and melatonin in the lipid membrane: (A) cholesterol, (B) melatonin.

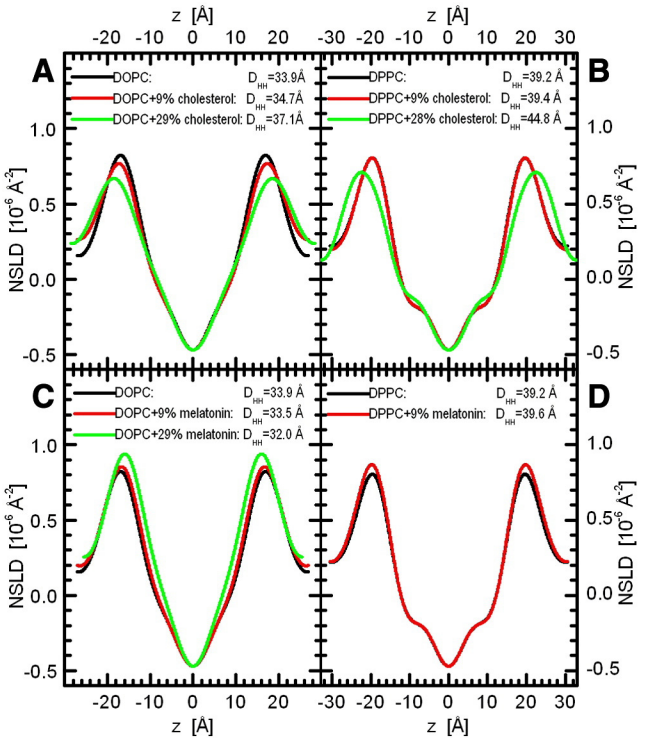

Fig. 4. Neutron Scattering Length Density (NSLD) profiles of DOPC bilayers with increasing concentrations of cholesterol (A) and melatonin (C), as well as DPPC with increasing concentrations of cholesterol (B) and melatonin (D). Profiles are of bilayers hydrated with 8% D_2O, and deliberately centered at z = 0 Å to allow for the direct comparison of the lipid head-group peak–peak distance (D_{HH}) of the different samples.

Fig. 4C and D show NSLD profiles for DOPC and DPPC bilayers, respectively, with increasing amounts of melatonin. In contrast to the effect by cholesterol, increasing amounts of melatonin in the lipid bilayer result in a progressive decrease in lipid bilayer thickness.

In the case of DOPC bilayers, for example, D_{HH} decreases from 33.9 Å in pure DOPC bilayers to 33.5 Å and 32.0 Å in DOPC bilayers with 9% and 29% melatonin, respectively (Fig. 4C). In DPPC bilayer with the lowest concentration of melatonin studied here (9%), it appears that melatonin causes only a slight increase in D_{HH} — i.e., pure DPPC has a D_{HH} of 39.2 Å, while DPPC with 9% melatonin increases to 39.6 Å. However, due to difficulties in preparing oriented DPPC samples, we were not able to obtain good quality data from DPPC bilayers with higher concentrations of melatonin. Therefore, we only used the data from ULV samples to report on how increasing amounts of cholesterol affected the D_{HH} of DPPC bilayers.

SANS data from ULV samples have been successfully used to study cholesterol's effects on DOPC bilayers [38,48]. As mentioned, SANS experiments were carried out using ULVs dispersed in 100% D_2O in order to improve the scattering contrast between the lipid bilayer and its surrounding water. By fitting the SANS data with an appropriate model, one can obtain NSLD profiles that differ from the ones obtained from oriented stacks of bilayers hydrated with 8% D_2O solution. In other words, in the ULV case with 100% D_2O, the water molecules are an integral part of the overall bilayer structure. As such, the obtained bilayer thickness (D_S) corresponds to the bilayer's steric thickness, which also includes the water molecules penetrating the bilayer's head-group region.

Analysis of the ULV cholesterol data obtained by SANS is in agreement with the data obtained from the diffraction experiments. Bilayer thickness D_S increases with increasing cholesterol concentration for both DOPC (Fig. 5A) and DPPC bilayers (Fig. 5B). In the case of DPPC bilayers (Fig. 5B), D_S increases from 57.0 Å, to 59.6 Å, and to 60.2 Å at 0%, 9% and 28% cholesterol, respectively. This result agrees well

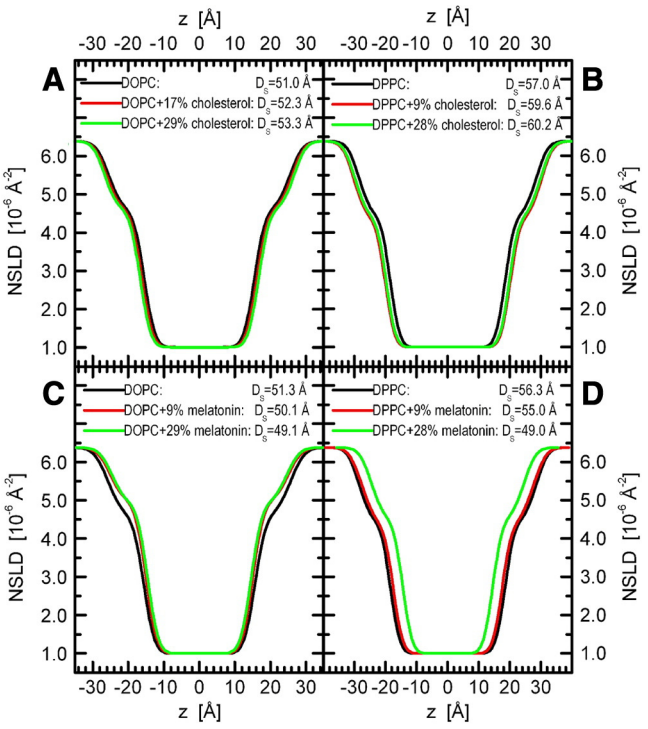

Fig. 5. Neutron Scattering Length Density profiles. The plots are results of fitting a smooth strip model to SANS data from DOPC (A) (adapted from [30]) and DPPC (B) (data from the N5 instrument) bilayers with increasing amounts of cholesterol. Panels C and D show the effect of melatonin on DOPC and DPPC bilayers, respectively (measured on the CG-3 Bio-SANS instrument). ULVs were extruded in 100% D_2O.

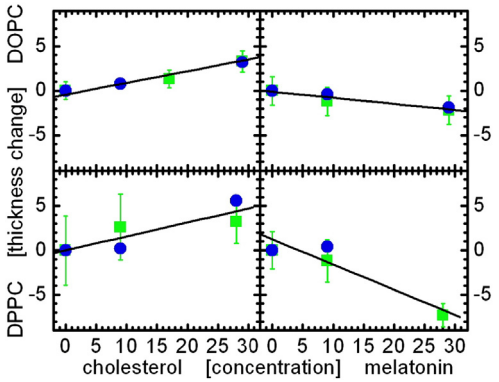

Fig. 6. Thicknesses of DOPC (top) and DPPC (bottom) bilayers upon the addition of cholesterol (left) and melatonin (right). Blue circles represent changes to the D_{HH} thickness obtained from SAND, while green squares correspond to changes in the D_S thickness obtained from SANS. Black lines are fits to the data.

with the known ordering effect that cholesterol has on saturated and monounsaturated phosphatidylcholine bilayers, where lipid chain ordering increases as a result of interactions with the rigid cholesterol molecule.

Importantly, our SANS studies of DOPC and DPPC bilayers with increasing amounts of melatonin show that both membranes undergo progressive thinning as a function of increasing amounts of melatonin (Fig. 5C and D respectively). In the case of pure DOPC, D_S has a value of 51.3 Å, which decreases to 50.1 Å and 49.1 Å upon the addition of 9% and 28% melatonin, respectively. A similar thinning trend is observed for the DPPC systems: the pure DPPC bilayer has a D_S of 56.3 Å, but the addition of 9% and 28% melatonin caused D_S to decrease, respectively to 55.0 Å and 49.0 Å. This result supports the notion that melatonin incorporates itself into the bilayer's head-group region, as shown in Fig. 3B. According to this scheme, melatonin acts as a spacer between lipid head-groups, causing the free volume in the bilayer's hydrocarbon region to increase. This free volume is then readily taken up by the disordered hydrocarbon chains at the expense of their effective length (i.e., reduced bilayer thickness).

Fig. 6 summarizes the different neutron data. Although it has been pointed out that the two bilayer thicknesses (i.e., D_{HH} and D_S) differ in their definition, their relative changes are directly comparable. Fig. 6 shows that there is very good agreement between D_{HH} and D_S as a function of increasing concentration of cholesterol or melatonin — i.e., increased amounts of cholesterol cause the bilayer to thicken, while melatonin has the exact opposite effect on bilayer thickness.

Lipid membrane thickness is a structural parameter that is needed to accurately determine other bilayer structural parameters and is directly related to lipid–lipid, and lipid–protein interactions in biomembranes. Our experimental results confirm the previously reported and well-known bilayer thickening effect induced by cholesterol (see Fig. 6). This, as a result of the hydrocarbon chains experiencing increased order due to their interactions with the rigid cholesterol molecules. Interestingly, our experimental results show, for the first time, that the addition of melatonin has the exact opposite effect, i.e., melatonin causes bilayer thinning (Fig. 6). This is most likely due to melatonin introducing disorder within the membrane by increasing the area per lipid as it incorporates itself among the lipid head-groups. This notion is also supported by the encroachment of water molecules deeper into the membrane (shown in Fig. 5C and D).

In order to further elucidate the structural details on the effect of melatonin and cholesterol on model lipid bilayers, we performed MD simulations. In agreement with our experimental SANS and SAND data, MD simulations show that cholesterol increases the acyl chain order of both DOPC and DPPC bilayers. In contrast to cholesterol, melatonin decreases the order in both bilayers (Fig. 7).

Fig. 7 illustrates the structure of DPPC and DOPC bilayers with and without melatonin. At 300 K, pure DPPC bilayers are in the gel phase (T_m of DPPC is 314 K). The figure clearly demonstrates that the presence of melatonin induces local disorder in the lipid tails, i.e., it melts the gel phase of the pure DPPC system (Fig. A vs Fig. 7B). The pure DPPC system has a number of lipids in the liquid phase (Fig. 7A). This is due to the fact that the time it takes to complete the phase transition is longer than the simulation time. The melatonin-containing system, however, is different (Fig. 7B): all of the melatonin containing regions are in the liquid phase, i.e., melatonin increases the fluidity of the system- the patches that do not contain melatonin remain in the gel phase. Since for DOPC the main transition temperature is lower, $T_m = 253$ K, it is already in the liquid state (Fig. 7C), therefore the effect of melatonin is readily apparent (Fig. 7D). To determine whether or not melatonin has a further fluidizing effect on DOPC we investigated the occurrence of bilayer thinning and changes to area per lipid.

MD data in Fig. 8 show that melatonin's (orange line) preferred location is just inside the crossover region describing the lipid head groups and the fatty acid chains. Fig. 8 shows that for DPPC (Fig. 8A) bilayers the peak density is decreased when melatonin is present. For DOPC (Fig. 8B), the peak density of the lipid tails is increased when melatonin is added (solid lines: no melatonin, dashed lines: with melatonin). In our DPPC simulations, the thickness of the membrane increased with the addition of melatonin from $D_{HH} = 39.8 \pm 0.1$ Å to 40.9 ± 0.5 Å. For DOPC, the thickness went from $D_{HH} = 37.0 \pm 0.1$ Å to 37.6 ± 0.5 Å after melatonin was added. The area of the pure DOPC bilayer was 67.4 ± 0.4 Å^2. The addition of melatonin increased this value to 69.4 ± 0.5 Å^2. The trends observed upon the addition of melatonin are in excellent agreement with our experimental results. In addition, the trends observed in neutron scattering upon addition of cholesterol are in perfect agreement with previous simulations [70,71]. Thus, we can conclude that the simulations provide an accurate picture of melatonin's location and effect for both DPPC and DOPC bilayers: melatonin interacts with the lipid head groups and does not penetrate into the hydrophobic core.

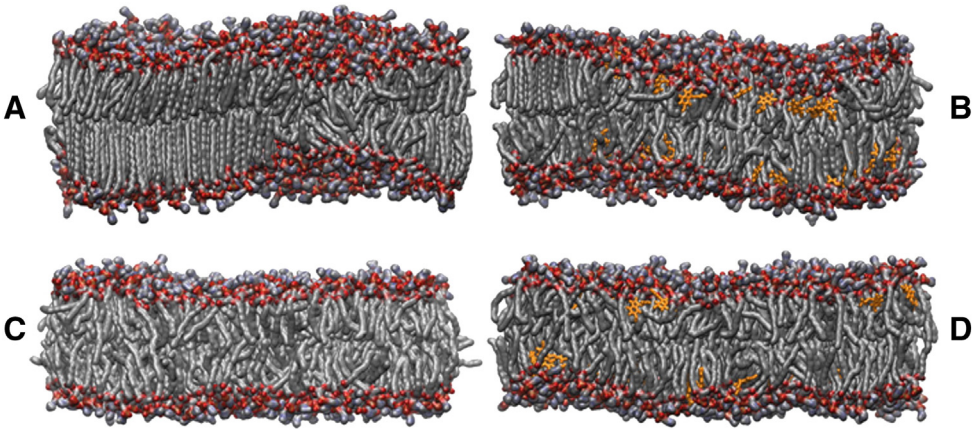

Fig. 7. Molecular Dynamics simulations of DPPC and DOPC bilayers with and without melatonin. DPPC (top) and DOPC (bottom) bilayers. Left: pure systems: A — DPPC, C — DOPC. Right: with melatonin: B — DPPC–mel, D — DOPC–mel. Melatonin molecules are shown in orange. Snapshots were taken after 400 ns of MD simulation at T = 300 K. The total simulation time for each system was 500 ns. Note the gel phase on the left hand side in the pure DPPC system (for DPPC, T_m = 314 K). Melatonin appears to enhance and maintain local fluidity. This is clearly visible in the DPPC membrane with melatonin (top right). Since the DOPC system is above its main phase transition (T_m = 253 K), the effects of melatonin are more subtle.

Both experimental and theoretical data are in good agreement and show that the effect of melatonin on bilayer thickness is opposite to that of cholesterol. Both experimental data and MD simulations show that cholesterol has an ordering effect, and increases bilayer thickness. In contrast to cholesterol, melatonin decreases the order and decreases the thickness of both bilayers, thus inducing increased fluidity in the model membrane. These observations may prove to be important for other studies on amyloid toxicity, as they may lend some insight into understanding the molecular mechanism of melatonin's protection in Alzheimer's disease. For example, melatonin levels in the body have been shown to decrease with age [72]. As Alzheimer's disease is more prevalent later in life, the effects of melatonin and cholesterol on lipid membrane become increasingly important as their amounts in membranes also change with age. Both cholesterol and melatonin have implications in amyloid toxicity and Alzheimer's progression in animal and cell studies [4,12] -although the molecular mechanism of their action is not well understood. Considering the role of the cell membrane in amyloid toxicity, it is also important to note that amyloid deposits are known to affect the synapse [73,74], where membrane fluidity is important for the propagation of the action potential signal from one neuron cell to another, which occurs through the fusion of synaptic vesicles. Our results can, for the first time, provide an understanding for the possible structural changes taking place within biological membranes. The effects of melatonin on membrane structure may have consequences similar to those of cholesterol reducing drugs. Studies have also shown that membrane cholesterol levels may regulate the toxic effects of amyloid beta, and that cholesterol reducing agents such as mevastatin, methyl-β-cyclodextrin or filipin, are able to reverse or diminish such toxic effects [75]. Melatonin has also been shown to significantly decrease cholesterol absorption and total cholesterol levels [76], in addition to its ability in reducing amyloid toxicity. Amyloid toxicity is directly related to the damage that amyloid produces in cell membranes. We have also shown previously [26] that amyloid binding, the first step in amyloid toxicity [77], is affected by cholesterol, i.e., the presence of cholesterol increases damage to the membrane, and in good agreement with data by Sheikh et al. [27]. Choucair et al. also reported that the phase of the lipid membrane is important for amyloid binding and demonstrated that the amyloid peptide preferentially binds to thicker and less fluid membranes [78].

In summary, we have shown that melatonin decreases bilayer thickness and increases the head group area, resulting in more fluid and disordered bilayers, in contrast to the well-known condensation effect induced by cholesterol. Based on our results, we hypothesize that melatonin may counteract cholesterol's membrane ordering effect, and thus may affect amyloid binding, which leads to membrane damage associated with amyloid toxicity. The present results help in understanding the mechanism by which cholesterol and melatonin may affect the properties of biological membranes, and they could be used to better comprehend the mechanism of interaction of membranes with amyloid peptides in relation to amyloid toxicity and AD.

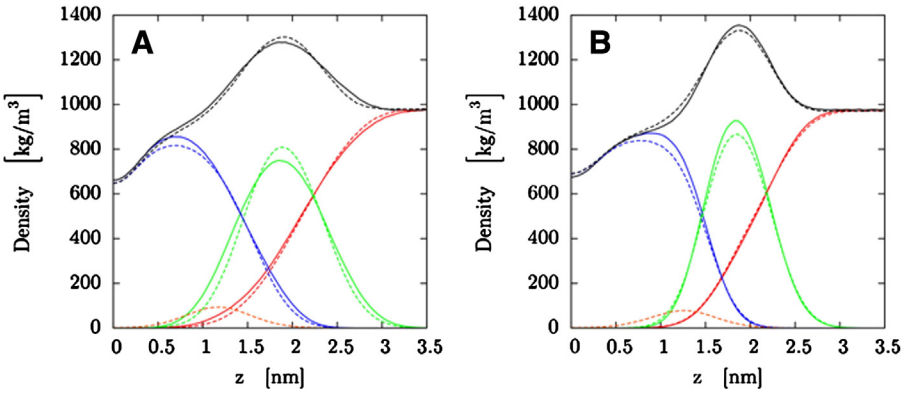

Fig. 8. Density profiles for one bilayer leaflet calculated from MD simulations of DPPC (A) and DOPC (B) membranes at T = 300 K. Zero denotes the membrane center. Pure membranes are represented by solid lines, and ones with melatonin by dashed lines. Black: total density, red: solvent, green: head groups, and blue: lipid tails, and orange: melatonin.

Acknowledgements

This work was supported by the Natural Science and Engineering Council of Canada (NSERC) [ZL, MK], Canadian Institute of Health Research (CIHR) [ZL], the University of Waterloo [MK, ZL], an NSERC Canada Graduate Scholarship and WIN Fellowship [ED], and a CIHR Graduate Scholarship and WIN Fellowship [YC]. The authors acknowledge the support of the Canadian Institute for Neutron Scattering (CINS) through the utilization of the Canadian Neutron Beam Centre (CNBC) facilities, and the office of Biological and Environmental Research at Oak Ridge National Laboratory's (ORNL) Center for Structural Molecular Biology (CSMB) through the utilization of facilities supported by the U.S. Department of Energy, managed by UT-Battelle, LLC under contract no. DE-AC05-00OR2275. JK is partially supported through ORNL's Laboratory Directed Research and Development (LDRD) program.

References

[1] F. Severcan, I. Sahin, N. Kazanci, Melatonin strongly interacts with zwitterionic model membranes—evidence from Fourier transform infrared spectroscopy and differential scanning calorimetry, Biochim. Biophys. Acta 1668 (2005) 215–222.
[2] D. Bongiorno, L. Ceraulo, M. Ferrugia, F. Filizzola, A. Ruggirello, V.T. Liveri, Localization and interactions of melatonin in dry cholesterol/lecithin mixed reversed micelles used as cell membrane models, J. Pineal Res. 38 (2005) 292–298.
[3] L. Mucke, D.J. Selkoe, Neurotoxicity of amyloid β-protein: synaptic and network dysfunction, Cold Spring Harb. Perspect. Med. 2 (2012) a006338.
[4] G. Di Paolo, T.-W. Kim, Linking lipids to Alzheimer's disease: cholesterol and beyond, Nat. Rev. Neurosci. 12 (2011) 284–296.
[5] R. Friedman, R. Pellarin, A. Caflisch, Amyloid aggregation on lipid bilayers and its impact on membrane permeability, J. Mol. Biol. 387 (2009) 407–415.
[6] G.P. Gellermann, T.R. Appel, A. Tannert, A. Radestock, P. Hortschansky, V. Schroeckh, C. Leisner, T. Lütkepohl, S. Shtrasburg, C. Röcken, M. Pras, R.P. Linke, S. Diekmann, M. Fändrich, Raft lipids as common components of human extracellular amyloid fibrils, Proc. Natl. Acad. Sci. U. S. A. 102 (2005) 6297–6302.
[7] M. Karasek, Melatonin, human aging, and age-related diseases, Exp. Gerontol. 39 (2004) 1723–1729.
[8] J.M. Olcese, C. Cao, T. Mori, M.B. Mamcarz, A. Maxwell, M.J. Runfeldt, L. Wang, C. Zhang, X. Lin, G. Zhang, G.W. Arendash, Protection against cognitive deficits and markers of neurodegeneration by long-term oral administration of melatonin in a transgenic model of Alzheimer disease, J. Pineal Res. 47 (2009) 82–96.
[9] S.A. Rosales-Corral, D. Acuña-Castroviejo, A. Coto-Montes, J.A. Boga, L.C. Manchester, L. Fuentes-Broto, A. Korkmaz, S. Ma, D.-X. Tan, R.J. Reiter, Alzheimer's disease: pathological mechanisms and the beneficial role of melatonin, J. Pineal Res. 52 (2012) 167–202.
[10] N. Dragicevic, N. Copes, G. O'Neal-Moffitt, J. Jin, R. Buzzeo, M. Mamcarz, J. Tan, C. Cao, J.M. Olcese, G.W. Arendash, P.C. Bradshaw, Melatonin treatment restores mitochondrial function in Alzheimer's mice: a mitochondrial protective role of melatonin membrane receptor signaling, J. Pineal Res. 51 (2011) 75–86.
[11] S. Benloucif, H.J. Burgess, E.B. Klerman, A.J. Lewy, B. Middleton, P.J. Murphy, B.L. Parry, V.L. Revell, Measuring melatonin in humans, J. Clin. Sleep Med. 4 (2008) 66–69.
[12] A.A. Kondratova, R.V. Kondratov, The circadian clock and pathology of the ageing brain, Nat. Rev. Neurosci. (2012), http://dx.doi.org/10.1038/nrn3208.
[13] J.J. Garcia, R.J. Reiter, J.M. Guerrero, G. Escames, B.P. Yu, C.S. Oh, A. Munoz-Hoyos, Melatonin prevents changes in microsomal membrane fluidity during induced lipid perodixation, FEBS Lett. 408 (1997) 297–300.
[14] A. Saija, A. Tomaino, D. Trombetta, M.L. Pellegrino, B. Tita, S. Caruso, F. Castelli, Interaction of melatonin with model membranes and possible implications in its photoprotective activity, Eur. J. Pharm. Biopharm. 53 (2002) 209–215.
[15] V.R. de Lima, M.S.B. Caro, M.I.B. Tavares, T.B. Creczynski-Pasa, Melatonin location in egg phosphatidylcholine liposomes: possible relation to its antioxidant mechanisms, J. Pineal Res. 43 (2007) 276–282.
[16] V.R. de Lima, M.S.B. Caro, M.L. Munford, B. Desbat, E. Dufourc, A.A. Pasa, T.B. Creczynski-Pasa, Influence of melatonin on the order of phosphatidylcholine-based membranes, J. Pineal Res. 49 (2010) 169–175.
[17] S.B. Akkas, S. Inci, F. Zorlu, F. Severcan, Melatonin affects the order, dynamics and hydration of brain membrane lipids, J. Mol. Struct. 834–836 (2007) 207–215.
[18] I. Sahin, F. Severcan, N. Kazancı, Melatonin induces opposite effects on order and dynamics of anionic DPPG model membranes, J. Mol. Struct. 834–836 (2007) 195–201.
[19] E.J.X. Costa, C.S. Shida, M.H. Biaggi, A.S. Ito, M.T. Lamy-Freund, How melatonin interacts with lipid bilayers — a study by fluorescence and ESR spectroscopies, FEBS Lett. 416 (1997) 103–106.
[20] J.J. García, R.J. Reiter, G.G. Ortiz, C.S. Oh, L. Tang, B.P. Yu, G. Escames, Melatonin enhances tamoxifen's ability to prevent the reduction in microsomal membrane fluidity induced by lipid peroxidation, J. Membr. Biol. 162 (1998) 59–65.
[21] Z. Feng, J.-T. Zhang, Protective effect of melatonin on beta-amyloid-induced apoptosis in rat astroglioma C6 cells and its mechanism, Free Radic. Biol. Med. 37 (2004) 1790–1801.
[22] B. Poeggeler, L. Miravalle, M.G. Zagorski, T. Wisniewski, Y.J. Chyan, Y. Zhang, H. Shao, T. Bryant-Thomas, R. Vidal, B. Frangione, J. Ghiso, M.A. Pappolla, Melatonin reverses the profibrillogenic activity of apolipoprotein E4 on the Alzheimer amyloid Abeta peptide, Biochemistry 40 (2001) 14995–15001.
[23] A. Galano, D.X. Tan, R.J. Reiter, Melatonin as a natural ally against oxidative stress: a physicochemical examination, J. Pineal Res. 51 (2011) 1–16.
[24] L. Puglielli, R.E. Tanzi, D.M. Kovacs, Alzheimer's disease: the cholesterol connection, Nat. Neurosci. 6 (2003) 345–351.
[25] S. Dante, T. Hauss, N.A. Dencher, Cholesterol inhibits the insertion of the Alzheimer's peptide Abeta(25–35) in lipid bilayers, Eur. Biophys. J. 35 (2006) 523–531.
[26] E. Drolle, R.M. Gaikwad, Z. Leonenko, Nanoscale electrostatic domains in cholesterol-laden lipid membranes create a target for amyloid binding, Biophys. J. 103 (2012) L27–L29.
[27] K. Sheikh, C. Giordani, J.J. McManus, M.B. Hovgaard, S.P. Jarvis, Differing modes of interaction between monomeric Aβ(1 – 40) peptides and model lipid membranes: an AFM study, Chem. Phys. Lipids 165 (2012) 142–150.
[28] C. Cecchi, D. Nichino, M. Zampagni, C. Bernacchioni, E. Evangelisti, A. Pensalfini, G. Liguri, A. Gliozzi, M. Stefani, A. Relini, A protective role for lipid raft cholesterol against amyloid-induced membrane damage in human neuroblastoma cells, Biochim. Biophys. Acta 1788 (2009) 2204–2216.
[29] T.A. Harroun, J. Katsaras, S.R. Wassall, Cholesterol hydroxyl group is found to reside in the center of a polyunsaturated lipid membrane, Biochemistry 45 (2006) 1227–1233.
[30] N. Kučerka, D. Marquardt, T.A. Harroun, M.-P. Nieh, S.R. Wassall, J. Katsaras, The functional significance of lipid diversity: orientation of cholesterol in bilayers is determined by lipid species, J. Am. Chem. Soc. 131 (2009) 16358–16359.
[31] T.P.W. McMullen, R.N.A.H. Lewis, R.N. McElhaney, Cholesterol–phospholipid interactions, the liquid-ordered phase and lipid rafts in model and biological membranes Curr. Opin. Colloid Interface Sci. 8 (2004) 459–468.
[32] H. Ohvo-Rekilä, B. Ramstedt, P. Leppimäki, J.P. Slotte, Cholesterol interactions with phospholipids in membranes, Prog. Lipid Res. 41 (2002) 66–97.
[33] A. Radhakrishnan, T.G. Anderson, H.M. McConnell, Condensed complexes, rafts, and the chemical activity of cholesterol in membranes, Proc. Natl. Acad. Sci. U. S. A. 97 (2000) 12422–12427.
[34] P.S. Niemela, S. Ollila, M.T. Hyvonen, M. Karttunen, I. Vattulainen, Assessing the nature of lipid raft membranes, PLoS Comput. Biol. 3 (2007) e34.
[35] C. Giordani, C. Wakai, K. Yoshida, E. Okamura, N. Matubayasi, M. Nakahara, Cholesterol location and orientation in aqueous suspension of large unilamellar vesicles of phospholipid revealed by intermolecular nuclear overhauser effect, J. Phys. Chem. B 112 (2008) 2622–2628.
[36] M. Bonn, S. Roke, O. Berg, L.B.F. Juurlink, A. Stamouli, M. Müller, A molecular view of cholesterol-induced condensation in a lipid monolayer, J. Phys. Chem. B 108 (2004) 19083–19085.
[37] R.A. Demel, B. De Kruyff, The function of sterols in membranes, Biochim. Biophys. Acta 457 (1976) 109–132.
[38] N. Kučerka, J. Pencer, M.-P. Nieh, J. Katsaras, Influence of cholesterol on the bilayer properties of monounsaturated phosphatidylcholine unilamellar vesicles, Eur. Phys. J. E 23 (2007) 247–254.
[39] N. Kučerka, D. Marquardt, T.A. Harroun, M.-P. Nieh, S.R. Wassall, D.H. De Jong, L.V. Schäfer, S.J. Marrink, J. Katsaras, Cholesterol in bilayers with PUFA chains: doping with DMPC or POPC results in sterol reorientation and membrane-domain formation, Biochemistry 49 (2010) 7485–7493.
[40] E. Sackmann, Biological Membranes Architecture and Function, in: R. Lipowski, E. Sackmann (Eds.), Structure and Dynamics of Membranes — From Cells to Vesicles, vol. 1A, 1995, pp. 1–65.
[41] J. Lemmich, K. Mortensen, J.H. Ipsen, T. Hønger, R. Bauer, O.G. Mouritsen, The effect of cholesterol in small amounts on lipid-bilayer softness in the region of the main phase transition, Eur. Biophys. J. 25 (1997) 293–304.
[42] S. Karmakar, V. Raghunathan, Cholesterol-induced modulated phase in phospholipid membranes, Phys. Rev. Lett. 91 (2003) 098102.
[43] D. Levy, K.A. Briggman, Cholesterol/phospholipid interactions in hybrid bilayer membranes, Langmuir 23 (2007) 7155–7161.
[44] N. Kučerka, J.F. Nagle, J.N. Sachs, S.E. Feller, J. Pencer, A. Jackson, J. Katsaras, Lipid bilayer structure determined by the simultaneous analysis of neutron and X-ray scattering data, Biophys. J. 95 (2008) 2356–2367.
[45] S.J. Marrink, A.H. de Vries, T. a Harroun, J. Katsaras, S.R. Wassall, Cholesterol shows preference for the interior of polyunsaturated lipid membranes, J. Am. Chem. Soc. 130 (2008) 10–11.
[46] S.A. Tristram-Nagle, Preparation of oriented, fully hydrated lipid samples for structure determination using X-ray scattering, Methods Mol. Biol. 400 (2007) 63–75.
[47] N. Kučerka, J. Pencer, J.N. Sachs, J.F. Nagle, J. Katsaras, Curvature effect on the structure of phospholipid bilayers, Langmuir 23 (2007) 1292–1299.
[48] N. Kučerka, M.-P. Nieh, J. Pencer, J.N. Sachs, J. Katsaras, What determines the thickness of a biological membrane, Gen. Physiol. Biophys. 28 (2009) 117–125.
[49] J. Als-Nielsen, D. McMorrow, Elements of Modern X-Ray Physics, John Wiley & Sons, Ltd., 2001
[50] D.L. Worcester, N.P. Franks, Structural analysis of hydrated egg lecithin and cholesterol bilayers II Neutron diffraction, J. Mol. Biol. 100 (1976) 359–378.
[51] M.-P. Nieh, Z. Yamani, N. Kucerka, J. Katsaras, D. Burgess, H. Breton, Adapting a triple-axis spectrometer for small angle neutron scattering measurements, Rev. Sci. Instrum. 79 (2008) 095102.
[52] G.W. Lynn, W. Heller, V. Urban, G.D. Wignall, K. Weiss, D.A.A. Myles, Bio-SANS—a dedicated facility for neutron structural biology at Oak Ridge National Laboratory, Physica B 385–386 (2006) 880–882.
[53] N. Kučerka, J.F. Nagle, S.E. Feller, P. Balgavý, Models to analyze small-angle neutron scattering from unilamellar lipid vesicles, Phys. Rev. E 69 (2004) 1–9.
[54] N. Kučerka, M.-P. Nieh, J. Katsaras, Small-angle scattering from homogenous and heterogeneous lipid bilayers, in: A. Iglič, H.T. Tien (Eds.), Advances in Planar Lipid Bilayers and Liposomes, Elsevier Inc., 2010, pp. 201–236.

[55] B. Hess, C. Kutzner, D. van der Spoel, E. Lindahl, GROMACS 4: algorithms for highly efficient, load-balanced, and scalable molecular simulation, J. Chem. Theory Comput. 4 (2008) 435–447.
[56] C. Oostenbrink, T.A. Soares, N.F.A. van der Vegt, W.F. van Gunsteren, Validation of the 53A6 GROMOS force field, Eur. Biophys. J. 34 (2005) 273–284.
[57] J. Wong-ekkabut, M. Karttunen, Assessment of common simulation protocols for simulations of nanopores, membrane proteins, and channels, J. Chem. Theory Comput. 8 (2012) 2905–2911.
[58] E.A. Cino, W.-Y. Choy, M. Karttunen, Comparison of secondary structure formation using 10 different force fields in microsecond molecular dynamics simulations, J. Chem. Theory Comput. 8 (2012) 2725–2740.
[59] M. Bachar, P. Brunelle, D.P. Tieleman, A. Rauk, Molecular dynamics simulation of a polyunsaturated lipid bilayer susceptible to lipid peroxidation, J. Phys. Chem. B 108 (2004) 7170–7179.
[60] T. Patko, A. Granovsky, N. Greeves, Quick Start and Usage Guide for Installing and Running Firefly Under MAX OS X (Release 71G for Leopard and Snow Leopard), 2010. 18.
[61] S. Miyamoto, P.A. Kollman, SETTLE: an analytical version of the SHAKE and RATTLE algorithm for rigid water models, J. Comput. Chem. 13 (1992) 952–962.
[62] B. Hess, H. Bekker, H.J.C. Berendsen, J.G.E.M. Fraaije, LINCS: a linear constraint solver for molecular simulations, J. Comput. Chem. 18 (1997) 1463–1472.
[63] U. Essmann, L. Perera, M.L. Berkowitz, T. Darden, H. Lee, L.G. Pedersen, A smooth particle mesh Ewald method, J. Chem. Phys. 103 (1995) 8577–8593.
[64] M. Karttunen, J. Rottler, I. Vattulainen, C. Sagui, Electrostatics in biomolecular simulations: where are we now and where are we heading? Curr. Top. Membr. 60 (2008) 49–89.
[65] M. Parrinello, A. Rahman, Polymorphic transitions in single crystals: a new molecular dynamics method, J. Appl. Phys. 52 (1981) 7182–7190.
[66] G. Bussi, D. Donadio, M. Parrinello, Canonical sampling through velocity rescaling, J. Chem. Phys. 126 (2007) 014101.
[67] P.L. Yeagle, Cholesterol and the cell membrane, Biochim. Biophys. Acta 822 (1985) 267–287.
[68] A. Léonard, C. Escrive, M. Laguerre, E. Pebay-Peyroula, W. Néri, T. Pott, J. Katsaras, E.J. Dufourc, Location of cholesterol in DMPC membranes. A comparative study by neutron diffraction and molecular mechanics simulation, Langmuir 17 (2001) 2019–2030.
[69] H. Martinez-Seara, T. Róg, M. Pasenkiewicz-Gierula, I. Vattulainen, M. Karttunen, R. Reigada, Interplay of unsaturated phospholipids and cholesterol in membranes: effect of the double-bond position, Biophys. J. 95 (2008) 3295–3305.
[70] M. Alwarawrah, J. Dai, J. Huang, A molecular view of the cholesterol condensing effect in DOPC lipid bilayers, J. Phys. Chem. B 114 (2010) 7516–7523.
[71] H. Martinez-Seara, T. Róg, M. Karttunen, I. Vattulainen, R. Reigada, Cholesterol induces specific spatial and orientational order in cholesterol/phospholipid membranes, PLoS One 5 (2010) e11162.
[72] R.L. Sack, A.J. Lewy, D.L. Erb, W.M. Vollmer, C.M. Singer, Human melatonin production decreases with age, J. Pineal Res. 3 (1986) 379–388.
[73] D.M. Walsh, D.J. Selkoe, Oligomers on the brain: the emerging role of soluble protein aggregates in neurodegeneration, Protein Pept. Lett. 11 (2004) 213–228.
[74] A. Lorenzo, B.A. Yankner, Amyloid fibril toxicity in Alzheimer's disease and diabetes, Ann. N. Y. Acad. Sci. 777 (1996) 89–95.
[75] A.Y. Abramov, M. Ionov, E. Pavlov, M.R. Duchen, Membrane cholesterol content plays a key role in the neurotoxicity of β-amyloid: implications for Alzheimer's disease, Aging Cell 10 (2011) 595–603.
[76] S.A.-R. Hussain, Effect of melatonin on cholesterol absorption in rats, J. Pineal Res. 42 (2007) 267–271.
[77] O. Simakova, N.J. Arispe, The cell-selective neurotoxicity of the Alzheimer's Abeta peptide is determined by surface phosphatidylserine and cytosolic ATP levels. Membrane binding is required for Abeta toxicity, J. Neurosci. 27 (2007) 13719–13729.
[78] A. Choucair, M. Chakrapani, B. Chakravarthy, J. Katsaras, L.J. Johnston, Preferential accumulation of Abeta(1–42) on gel phase domains of lipid bilayers: an AFM and fluorescence study, Biochim. Biophys. Acta 1768 (2007) 146–154.